BIBECHANA
Vol. 21, No. 2, August 2024, 83-94

ISSN 2091-0762 (Print), 2382-5340 (Online)
Journal homepage: `http://nepjol.info/index.php/BIBECHANA`
Publisher: Dept. of Phys., Mahendra Morang A. M. Campus (Tribhuvan University)Biratnagar

Theoretical exploration of thermodynamic characteristics in lead-free liquid alloys: Zn-Bi-In System

Sanjay Kumar Sah[1,3,*], **Indu Shekhar Jha**[2], **Ishwar Koirala**[1]

[1] *Central Department of Physics, Tribhuvan University, Kirtipur, Kathmandu, Nepal*
[2] *Department of Physics, M.M.A.M. Campus, Tribhuvan University, Biratnagar, Nepal*
[3] *Dept. of Physics, Birendra Multiple Campus, Tribhuvan University, Bharatpur, Nepal*

[*] Corresponding author. Email: `sanjay.sah@bimc.tu.edu.np`

Abstract

The calculations of Zn activities in the ternary liquid solder alloy Zn-Bi-In at 873 K were conducted through the application of the Molecular Interaction Volume Model (MIVM). The calculated values were compared to experimental data for four different cross-sectional examinations, namely for the bismuth-to-indium ratios (x_{Bi}: x_{In}) of 1:2, 1:1, 2:1, and 9:1. Moreover, the integral excess free energy of these ternary liquid alloys was assessed using the same model parameters in order to test their validity. Then, the values were compared to the relevant experimental data reported in the literature that was already in existence. A satisfactory concordance has been observed between the theoretical predictions and the experimental findings.

Keywords
Activity; Integral excess free energy; Solder alloys; Ternary liquid alloys; Molecular interaction volume model.

Article information
Manuscript received: November 21, 2023; Revised: December 26, 2023; Accepted: January 14, 2024
DOI `https://doi.org/10.3126/bibechana.v21i2.60097`

1 Introduction

It is possible to investigate the thermodynamic characteristics of different alloys through experimental measurements. But the experimental methods are much more costly and time-consuming, given that numerous measurements and advanced instruments are required. Furthermore, experimental data are scarce for alloys with multiple components. As such, it is difficult to obtain all thermodynamic data solely through experimentation [1–4]

Therefore, it is more advantageous to obtain the data through theoretical means. Lead-based systems have been traditionally preferred for soldering due to their lower cost and lower melting point. However, lead is a toxic metal and has adverse effects on the environment. It can contaminate the soil, water, and air [5–8]. Currently, there is a worldwide agreement to outlaw lead use. Therefore, the development of soldering alternatives without lead has emerged as a crucial topic in the field of electronics [8]. In addition to comparable melting points, the new alloys ought to possess other qualities like low cost, non-toxicity, fatigue and corrosion resistance, and wetting qualities. Thus, researchers have attempted to replace lead in solder alloys multiple times [8].

Zinc, bismuth, and indium can be chosen as beneficial materials for lead-free solder alloys due to several advantageous properties and characteristics. These are less toxic than lead, making them more environmentally friendly alternatives. Alloys of those materials can have a relatively lower melting point and often exhibit good wetting properties. They also exhibit good thermal fatigue resistance, contributing to the reliability and durability of solder joints, especially in applications where the temperature may vary. Mainly, zinc imparts corrosion resistance to the solder alloys, and it is a relatively inexpensive material that is readily available [9].

Various alloy systems have been developed as alternatives to traditional Sn-Pb (tin-lead) alloys, particularly for electronic soldering applications. Here are examples of binaries, ternaries, and higher alloy systems: Tin-Silver (Sn-Ag), Gold-Tin (Au-Sn), Tin-Copper (Sn-Cu), Tin-Silver-Copper (Sn-Ag-Cu), Aluminium-Tin-Zinc (Al-Sn-Zn), Tin-Antimony-Bismuth (Sn-Sb-Bi), Tin-Silver-Copper-Antimony (Sn-Ag-Cu-Sb), and Tin-Silver-Copper-Zinc (Sn-Ag-Cu-Zn), etc. [6–8, 10–15]. Several geometric models are widely used in predicting the thermodynamic properties of binary, ternary, and other systems of higher complexity. These models include Muggianu, Kohler, Chou, Collinet, R-K equations, the Kaptay model, etc. [16–18]. MIVM is superior to other models because of the way it is formulated, which requires fewer fitting parameters (only two) [19]. MIVM has the unique capability to simultaneously represent the influences of the microstate number of molecular configuration (entropy) and molecular interaction (enthalpy) on excess Gibbs energy. Over the past two decades, the precision and dependability of MIVM in predicting the properties of liquid alloys have been substantiated [20, 21]. MIVM is a model characterized by two parameters. One of the model's most important features is its capability to forecast liquid alloy thermodynamic properties in a system of multiple component mixtures using typical physical parameters of metals in liquid form and binary infinite dilution activity coefficients alone [1].

Thermodynamic activities of the components of ternary liquid alloys Indium-Bismuth-Tin (In-Bi-Sn), Tin-Gold-Copper (Sn-Au-Cu), and Zinc-Indium-Tin (Zn-In-Sn), along with their excess Gibbs free energy of mixing, have been performed by Sah et al. [9, 22]. A comprehensive thermodynamic representation of the complete ternary system Bi-In-Zn was achieved through CALPHAD modeling, focusing on the Gibbs energy of the liquid phase [23]. Utilizing a Calvet-type microcalorimeter and the drop calorimetric technique, the integral enthalpies of mixing for liquid Bi-In-Zn alloys at 773 K were determined [24]. But there is only restricted information accessible through this system. The thermodynamic characteristics of the Bi-In-Zn ternary system were established utilizing the electromotive force (EMF) method, employing a liquid electrolyte, as outlined by the reference [25]. Nevertheless, there is presently no documentation in the literature regarding the computation of their integral excess free energy. Hence, in this study, the molecular interaction volume model was utilized to determine the thermodynamic activities of the Zn component in the ternary liquid alloys Zn-Bi-In at 873 K for the four cross-sections, namely $\mathrm{x_{Bi}}$: $\mathrm{x_{In}}$ = 1:2, 1:1, 2:1, and 9:1. Moreover, the theoretical model was employed to compute the integral excess Gibbs free energy of mixing for Zn-Bi-In at 873 K, considering varying concentrations of Zn ($\mathrm{x_{Zn}}$) across all those cross-sections.

2 Methodology

The MIVM model states that liquid molecules behave differently from both gas molecules, which move randomly all the time, and solid molecules, which oscillate continuously at one spot but move between molecular cells in a non-random way. The cells are both mobile and identical, and the molecules in the center and those closest to them can be interchanged [26]. MIVM is a fluid model based on statistical thermodynamics that takes into consideration the inherent physical characteristics of the individual pure metals that make up the alloy. Molar volume (Vm) and the liquid phase's first coordination number (Z) are specifically taken into account, which are dependent on temperature [19]. The excess molar Gibbs energy of the liquid binary mixture, i-j, is expressed as per Dong Ping Tao in 2000 based on the molecular interaction volume model [27]:

$$\Delta G^{XS} = RT\left\{x_i \ln\left(\frac{V_{mi}}{x_iV_{mi}+x_jV_{mj}A_{ji}}\right) + x_j\ln\left(\frac{V_{mj}}{x_jV_{mj}+x_iV_{mi}A_{ij}}\right) - \frac{x_ix_j}{2}\left(\frac{Z_iA_{ji}\ln A_{ji}}{x_i+x_jA_{ji}} + \frac{Z_jA_{ij}\ln A_{ij}}{x_j+x_iA_{ij}}\right)\right\} \tag{1}$$

In this context, V_{mi} and V_{mj} represent the molar volumes, while x_i and x_j denote the molar fractions of components i and j, respectively. $\mathrm{A_{ji}}$ and $\mathrm{A_{ij}}$ are the interaction parameters associated with the pair potential energy for binary liquid alloys. $\mathrm{Z_i}$ and $\mathrm{Z_j}$ are the first coordination numbers specific to the $\mathrm{i_{th}}$ and $\mathrm{j_{th}}$ component metals in binary liquid alloys. T stands for the absolute temperature and R represents the gas constant. In the case of a binary liquid alloy, the activity coefficients of components i and j, denoted as γ_i and γ_j, are expressed as per Tao in 2008 [26] as:

$$\ln\gamma_i = \ln\left(\frac{V_{mi}}{x_iV_{mi}+x_jV_{mj}A_{ji}}\right) + x_j\left(\frac{V_{mj}A_{ji}}{x_iV_{mi}+x_jV_{mj}A_{ji}} - \frac{V_{mi}A_{ij}}{x_jV_{mj}+x_iV_{mi}A_{ij}}\right) - \frac{x_j^2}{2}\left[\frac{Z_iA_{ji}^2\ln A_{ji}}{(x_i+x_jA_{ji})^2} + \frac{Z_jA_{ij}\ln A_{ij}}{(x_j+x_iA_{ij})^2}\right] \tag{2}$$

$$\ln\gamma_j = \ln\left(\frac{V_{mj}}{x_jV_{mj}+x_iV_{mi}A_{ij}}\right) - x_i\left(\frac{V_{mj}A_{ji}}{x_iV_{mi}+x_jV_{mj}A_{ji}} - \frac{V_{mi}A_{ij}}{x_jV_{mj}+x_iV_{mi}A_{ij}}\right) - \frac{x_i^2}{2}\left[\frac{Z_jA_{ij}^2\ln A_{ij}}{(x_j+x_iA_{ij})^2} + \frac{Z_iA_{ji}\ln A_{ji}}{(x_i+x_jA_{ji})^2}\right] \tag{3}$$

For the system of higher orders, i.e., for a multicomponent mixture, Eq. (1) becomes [27]:

$$\Delta G^{XS} = RT\left\{\sum_{i=1}^{N} x_i\ln\frac{V_{mi}}{\sum_{j=1}^{N} x_jV_{mj}A_{ji}} - \frac{1}{2}\sum_{i=1}^{N} Z_ix_i\left(\frac{\sum_{j=1}^{N} x_jA_{ji}\ln A_{ji}}{\sum_{k=1}^{N} x_kA_{ki}}\right)\right\} \tag{4}$$

Where N is the number of components in a mixture.

The formula for the activity coefficient of the $\mathrm{i^{th}}$ component, γ_i, is provided in the work of Tao in 2008 [26] by:

$$\ln\gamma_i = 1 + \ln\frac{V_{mi}}{\sum_{j=1}^{N} x_jV_{mj}A_{ji}} - \sum_{k=1}^{N}\frac{x_kV_{mi}A_{ik}}{\sum_{j=1}^{N} x_jV_{mj}A_{jk}} - \frac{1}{2}\left\{\frac{Z_i\sum_{j=1}^{N} x_jA_{ji}\ln A_{ji}}{\sum_{l=1}^{N} x_lA_{li}} + \sum_{j=1}^{N}\frac{Z_jx_jA_{ij}}{\sum_{l=1}^{N} x_lA_{lj}} \times \left(\ln A_{ij} - \frac{\sum_{t=1}^{N} x_tA_{tj}\ln A_{tj}}{\sum_{l=1}^{N} x_lA_{lj}}\right)\right\} \tag{5}$$

The formula for Zi is presented in a publication by Tao in 2008 [26] by:

$$\mathrm{Z_i} = \frac{4\sqrt{2\pi}}{3}\left(\frac{\mathrm{r_{mi}^3 - r_{oi}^3}}{\mathrm{r_{mi} - r_{oi}}}\right)\rho_{\mathrm{i}}\mathrm{r_{mi}}\exp\left(\frac{\Delta\mathrm{H_{mi}}\left(\mathrm{T_{mi}} - \mathrm{T}\right)}{\mathrm{Z_cRTT_{mi}}}\right) \tag{6}$$

The molecular number density can be determined using the equation, , where Ni = 0.6022 represents the molecular number. The melting temperature and melting enthalpy are indicated by $\mathrm{T_{mi}}$ and ΔH_{mi}, respectively. Z_c signifies a close-packed coordination, with a value of 12 for certain liquid metals. $\mathrm{r_{oi}}$ represents the first peak value of the radial distribution function, and $\mathrm{r_{mi}}$ is the initial value of the radial distribution function, whose expressions are as follows:

$$\mathrm{r_{oi}} = 0.918\,\mathrm{d_{covi}} \tag{7}$$

And

$$\mathrm{r_{mi}} = \sigma_{\mathrm{i}} \tag{8}$$

Here d_{covi} and σ_i represent the atomic covalent diameter and atomic diameter, respectively.

The interaction parameters associated with pair potential energy are denoted by A_{ji} and A_{ij}, according to the findings of Tao et al. in 2002 as [33]:

$$\mathrm{A_{ji}} = \exp\left(-\frac{\varepsilon_{\mathrm{ji}} - \varepsilon_{\mathrm{ii}}}{\mathrm{KT}}\right) \quad ; \quad \mathrm{A_{ij}} = \exp\left(-\frac{\varepsilon_{\mathrm{ij}} - \varepsilon_{\mathrm{ji}}}{\mathrm{KT}}\right) \tag{9}$$

Here $\varepsilon_{\mathrm{ji}}$or $\varepsilon_{\mathrm{ij}}, \varepsilon_{\mathrm{ii}}$ and $\varepsilon_{\mathrm{jj}}$ represent the pair potential energies for i-j, i-i, and j-j interactions, respectively, with K being the Boltzmann constant.

The activity coefficients γ_i^∞ and γ_j^∞ for components i and j in binary liquid alloys are given in the limit of infinite dilution [26] as:

$$\ln\gamma_i^\infty = 1 - \ln\left(\frac{V_{mj}A_{ji}}{V_{mi}}\right) - \frac{V_{mi}A_{ij}}{V_{mj}} - \frac{1}{2}\left(Z_i\ln A_{ji} + Z_jA_{ij}\ln A_{ij}\right) \tag{10}$$

$$\ln\gamma_j^{\infty} = 1 - \ln\left(\frac{V_{mi}A_{ij}}{V_{mj}}\right) - \frac{V_{mj}A_{ji}}{V_{mi}} \\ - \frac{1}{2}\left(Z_j \ln A_{ij} + Z_i A_{ji}\ln A_{ji}\right) \tag{11}$$

Equations (10) and (11) must be solved using the Newton-Raphson method in order to determine $\mathrm{A_{ji}}$ and $\mathrm{A_{ij}}$. These starting values are then adjusted when component activities in liquid binary alloys are calculated using equations (2) and (3). Odusote et al. (2017) [28] explained that once the appropriate values of $\mathrm{A_{ji}}$ and $\mathrm{A_{ij}}$ at a particular temperature is established, their corresponding values at different temperatures can also be derived.

Considering the Zn-Bi-In ternary liquid alloy as the 1-2-3 system, the activity coefficient of the first metal, denoted as γ_1, in the system can be determined using equation (5), as explained by Tao in 2001 as [29]:

$$\begin{aligned} \ln\gamma_1 = {} & 1 + \ln\left(\frac{V_{m1}}{x_1V_{m1} + x_2V_{m2}A_{21} + x_3V_{m3}A_{31}}\right) \\ & - \frac{x_1V_{m1}}{x_1V_{m1} + x_2V_{m2}A_{21} + x_3V_{m3}A_{31}} \\ & - \frac{x_2V_{m1}A_{12}}{x_1V_{m1}A_{12} + x_2V_{m2} + x_3V_{m3}A_{32}} \\ & - \frac{x_3V_{m1}A_{13}}{x_1V_{m1}A_{13} + x_2V_{m2}A_{23} + x_3V_{m3}} \\ & - \frac{1}{2}\Bigg(\frac{Z_1\left(x_2A_{21} + x_3A_{31}\right)\left(x_2A_{21}\ln A_{21} + x_3A_{31}\ln A_{31}\right)}{\left(x_1 + x_2A_{21} + x_3A_{31}\right)^2} \\ & + \frac{Z_2x_2A_{12}\left[\left(x_2 + x_3A_{32}\right)\ln A_{12} - x_3A_{32}\ln A_{32}\right]}{\left(x_1A_{12} + x_2 + x_3A_{32}\right)^2} \\ & + \frac{Z_3x_3A_{13}\left[\left(x_2A_{23} + x_3\right)\ln A_{13} - x_2A_{23}\ln A_{23}\right]}{\left(x_1A_{13} + x_2A_{23} + x_3\right)^2}\Bigg) \end{aligned} \tag{12}$$

Likewise, the surplus Gibbs free energy of mixing, ΔG^{XS} for Zn-Bi-In ternary liquid alloys can be derived from equation (4) as:

$$\Delta G^{\mathrm{XS}} = RT\left\{\begin{array}{l} \mathrm{x_1}\ln\left(\frac{\mathrm{V_{m1}}}{\mathrm{x_1\ V_{m1}+x_2\ V_{m2}\ A_{21}+x_3\ V_{m3}\ A_{31}}}\right) \\ +\mathrm{x_2}\ln\left(\frac{\mathrm{V_{m2}}}{\mathrm{x_1\ V_{m1}\ A_{12}+x_2\ V_{m2}+x_3\ V_{m3}\ A_{32}}}\right) \\ +\mathrm{x_3}\ln\left(\frac{\mathrm{V_{m3}}}{\mathrm{x_1\ V_{m1}\ A_{13}+x_2\ V_{m2}\ A_{23}+x_3\ V_{m3}}}\right) \\ -\frac{1}{2}\Bigg[\frac{\mathrm{Z_1x_1(x_2\ A_{21}\ln A_{21}+x_3\ A_{31}\ln A_{31})}}{\mathrm{(x_1+x_2\ A_{21}+x_3\ A_{31})}} \\ +\frac{\mathrm{Z_2x_2(x_1\ A_{12}\ln A_{12}+x_3\ A_{32}\ln A_{32})}}{\mathrm{(x_1\ A_{12}+x_2+x_3\ A_{32})}}+ \\ \frac{\mathrm{Z_3x_3(x_1\ A_{13}\ln A_{13}+x_2\ A_{23}\ln A_{23})}}{\mathrm{(x_1\ A_{13}+x_2\ A_{23}+x_3)}} \end{array}\right\} \tag{13}$$

3 Results and Discussion

The required input parameters are outlined in Table 1. The values of the interaction parameters of potential energy ($\mathrm{A_{ji}}$ and $\mathrm{A_{ij}}$) for the binary alloys, as well as the first coordination numbers ($\mathrm{Z_i}$ and $\mathrm{Z_j}$) for the components of the binary systems, are provided in Table 2. Coordination numbers have been computed using the formula provided in Eq. (6). By plugging in the values of $\mathrm{V_{m1}}$, $\mathrm{V_{m2}}$, $\mathrm{V_{m3}}$, $\mathrm{Z_1}$, $\mathrm{Z_2}$, $\mathrm{Z_3}$, $\mathrm{A_{12}}$, $\mathrm{A_{21}}$, $\mathrm{A_{13}}$, $\mathrm{A_{31}}$, $\mathrm{A_{23}}$, and $\mathrm{A_{32}}$ into equations (12) and (13), the activities of the Zn component in the Zn-Bi-In systems at 873 K and the excess Gibbs free energy of mixing, ΔG^{XS}, for those ternary liquid alloys at 873 K were computed for all four cross-sections of $\mathrm{x_{Bi}}$: $\mathrm{x_{In}}$ = 1:2, 1:1, 2:1, and 9:1. The results were then compared with the corresponding experimental values [25], as illustrated in Table 3 and Table 4 and depicted in Figures 1, 2, 3, and 4, respectively.

Table 1: Certain input parameters [30].

Metal	ΔH_{mi} [KJ/mol]	r_{oi} [$\times 10^{-8}$ cm]	r_{mi} [$\times 10^{-8}$ cm]	V_{mi} [cm^3/mol]
Zn	7.322	2.16	2.66	$9.94(1 + 1.50 \times 10^{-4}(T - 693))$
Bi	11.30	2.78	3.34	$20.80(1 + 1.17 \times 10^{-4}(T - 544))$
In	3.263	2.70	3.14	$16.30(1 + 0.97 \times 10^{-4}(T - 430))$

Table 2: Values of A_{ij}, A_{ji}, Z_i, and Z_j computed for a range of temperature conditions in binary alloys.

i-j	T [K]	A_{ij}	A_{ji}	Z_i	Z_j
$Bi - Zn$	873	1.1106	0.4125	8.1043	8.9699
$In - Zn$	873	1.008	0.7123	9.1631	8.9699
$Bi - In$	873	1.3774	0.7545	8.1043	9.1631

Table 3: Experimental and theoretical data on Zn activities in Zn-Bi-In ternary liquid alloys at 873 K.

x_{Zn}	x_{Bi}	x_{In}	$a_{Zn}, Th.$	E(mV)	$a_{Zn}, Exp.*$	$\lvert a_{Zn}, Th. - a_{Zn}, Exp.*\rvert$
$x_{Bi} : x_{In} = 1 : 2$						
0.00000	——-	——-	0.00000	——-	——-	——-
0.09900	0.30033	0.60067	0.30081	43.3253	0.31605	0.01524
0.20410	0.26530	0.53060	0.53972	23.2751	0.53859	0.00113
0.29920	0.23360	0.46720	0.69326	14.7078	0.67636	0.01690
0.40160	0.19946	0.39894	0.80280	11.456	0.73744	0.06536
0.49120	0.16960	0.33920	0.86063	6.6841	0.83719	0.02344
0.59730	0.13423	0.26847	0.89566	4.584	0.88526	0.01040
0.69580	0.10140	0.20280	0.90833	3.3761	0.91415	0.00582
0.79760	0.06746	0.13494	0.91601	3.0964	0.92097	0.00496
0.89730	0.03423	0.06847	0.93611	1.987	0.94854	0.01243
1.00000	0.00000	0.00000	1.00000	——-	——-	——-
$x_{Bi} : x_{In} = 1 : 1$						
0.00000	——-	——-	0.00000	——-	——-	——-
0.09940	0.45030	0.45030	0.30020	44.5091	0.30626	0.00606
0.2017	0.39915	0.39915	0.54240	22.7301	0.54645	0.00405
0.30240	0.34880	0.34880	0.71736	13.1409	0.70513	0.01223
0.39980	0.30010	0.30010	0.83199	7.88080	0.81097	0.02102
0.50040	0.24980	0.24980	0.90211	5.05520	0.87424	0.02787
0.59860	0.20070	0.20070	0.93336	3.4939	0.91129	0.02207
0.70060	0.14970	0.14970	0.93997	2.8001	0.92826	0.01171
0.80020	0.09990	0.09990	0.93665	2.1225	0.94513	0.00848
0.89930	0.05035	0.05035	0.94450	1.5482	0.95967	0.01517
1.00000	0.00000	0.00000	1.00000	——-	——-	——-
$x_{Bi} : x_{In} = 2 : 1$						
0.00000	——-	——-	0.00000	——-	——-	——-
0.10030	0.59980	0.29990	0.29176	45.3836	0.29922	0.00746
0.19910	0.53394	0.26696	0.52902	24.8022	0.51716	0.01186
0.30060	0.46627	0.23313	0.71723	14.2952	0.68382	0.03341
0.40010	0.39994	0.19996	0.84696	8.6099	0.79540	0.05156
0.49980	0.33347	0.16673	0.92624	4.5123	0.88695	0.03929
0.60090	0.26607	0.13303	0.96254	4.5873	0.88518	0.07736
0.70020	0.19987	0.09993	0.96658	2.8197	0.92777	0.03881
0.80210	0.13194	0.06596	0.95496	1.6984	0.95585	0.00089
0.90070	0.06620	0.03310	0.95209	1.451	0.96215	0.01006
1.00000	0.00000	0.00000	1.00000	——-	——-	——-
$x_{Bi} : x_{In} = 9 : 1$						
0.00000	——-	——-	0.00000	——-	——-	——-
0.10040	0.80964	0.08996	0.26752	49.751	0.26642	0.00110
0.20050	0.71955	0.07995	0.50356	28.031	0.47462	0.02894
0.30040	0.62964	0.06996	0.69851	16.1431	0.65104	0.04747
0.39800	0.54180	0.06020	0.84287	9.2727	0.78151	0.06136
0.50050	0.44955	0.04995	0.94218	4.7572	0.88119	0.06099
0.60020	0.35982	0.03998	0.98945	1.8141	0.95291	0.03654
0.70020	0.26982	0.02998	0.99628	1.6721	0.95651	0.03977
0.80020	0.17982	0.01998	0.97816	1.2784	0.96658	0.01158
0.90010	0.08991	0.00999	0.96181	0.90330	0.97627	0.00108
1.00000	0.00000	0.00000	1.00000	——-	——-	——-

Experimental [25] S_i = ± 3.10 %, S_i^*= ± 0.0302

Table 4: Experimental and theoretical data on Zn-Bi-In ternary liquid alloys' excess Gibbs free energy mixing at 873 K.

x_{Zn}	x_{Bi}	x_{In}	ΔG^{XS}Th. [J/mol]	ΔG^{XS}Exp.* [J/mol]
$x_{Bi} : x_{In} = 1 : 2$				
0.0000	0.3333	0.6667	-1549.8	-1793.0
0.1000	0.2250	0.6750	-373.4	-143.0
0.2000	0.2667	0.5333	355.8	692.0
0.3000	0.2333	0.4667	1133.4	1429.0
0.4000	0.2000	0.4000	1763.4	2025.0
0.5000	0.1667	0.3333	2216.0	2417.0
0.6000	0.1333	0.2667	2453.4	2566.0
0.7000	0.1000	0.2000	2427.1	2460.0
0.8000	0.0667	0.1333	2073.4	2103.0
0.9000	0.0333	0.0667	1304.8	1464.0
1.0000	0.0000	0.0000	0.0	0.0
$x_{Bi} : x_{In} = 1 : 1$				
0.0000	0.5000	0.5000	-1635.1	-1916.0
0.1000	0.4500	0.4500	-633.3	-291.0
0.2000	0.4000	0.4000	281.1	560.0
0.3000	0.3500	0.3500	1087.3	1337.0
0.4000	0.3000	0.3000	1758.5	1984.0
0.5000	0.2500	0.2500	2260.8	2426.0
0.6000	0.2000	0.2000	2550.1	2618.0
0.7000	0.1500	0.1500	2567.7	2544.0
0.8000	0.1000	0.1000	2233.4	2209.0
0.9000	0.0500	0.0500	1433.8	1568.0
1.0000	0.0000	0.0000	0.0	0.0
$x_{Bi} : x_{In} = 2 : 1$				
0.0000	0.6667	0.3333	-1368.1	-1547.0
0.1000	0.6750	0.2250	-230.3	-39.0
0.2000	0.5333	0.2667	443.2	746.0
0.3000	0.4667	0.2333	1224.6	1482.0
0.4000	0.4000	0.2000	1887.7	2094.0
0.5000	0.3333	0.1667	2396.0	2501.0
0.6000	0.2667	0.1333	2700.8	2658.0
0.7000	0.2000	0.1000	2734.2	2562.0
0.8000	0.1333	0.0667	2401.5	2227.0
0.9000	0.0667	0.0333	1563.3	1619.0
1.0000	0.0000	0.0000	0.0	0.0
$x_{Bi} : x_{In} = 9 : 1$				
0.0000	0.9000	0.1000	-512.1	-504.0
0.1000	0.8100	0.0900	266.3	811.0
0.2000	0.7200	0.0800	1003.7	1414.0
0.3000	0.6300	0.0700	1679.0	2001.0
0.4000	0.5400	0.0600	2263.9	2506.0
0.5000	0.4500	0.0500	2719.8	2851.0
0.6000	0.3600	0.0400	2993.4	2981.0
0.7000	0.2700	0.0300	3007.9	2871.0
0.8000	0.1800	0.0200	2650.2	2506.0
0.9000	0.0900	0.0100	1744.6	1812.0
1.0000	0.0000	0.0000	0.0	0.0

Table 4 indicates that the theoretical and experimental values [25] of the excess free energy of mixing in Zn-Bi-In liquid alloys at 873 K exhibit reasonable agreement, albeit with some discrepancies. The highest errors are observed at $\mathrm{x_{Zn}} = 0.1$ for all four cross-sections, specifically $\mathrm{x_{Bi}}$: $\mathrm{x_{In}}$ = 1:2, 1:1, 2:1, and 9:1.

From the experimental work of Knott et al. [25], the activity of the component Zn in the Zn-Bi-In ternary liquid alloy can be determined by a relation given in Eq. (14).

$$\overline{\Delta G_{Zn}} = \mathrm{RT}\ln a_{Zn} = -\mathrm{zFE} \qquad (14)$$

where $\overline{\Delta G_{\mathrm{Zn}}}$ is the change in Gibbs free energy for the Zn component, z is the valency of Zn, F represents Faraday's constant (i.e., 96486 Coulomb/mol), R represents the molar gas constant and E represents the measured EMF of the cell, whose values for all the cross-sections of Bi and In have been taken from the reference [25].

Based on the information in Table 3, the mean relative error ($\mathrm{S_i}$) and mean standard deviation (S_i^*) were computed to precisely determine the extent of the difference between the experimental and predicted data. To calculate the average relative error, equation (15) can be used.

$$S_i = \pm\frac{100}{n}\sum_{i=1}^{n}\left|\frac{a_{i,\mathrm{Th.}} - a_{i,\mathrm{Exp.}^*}}{a_{i,\mathrm{Exp.}^*}}\right| \qquad (15)$$

Eq. (16) can be used to get the mean standard deviation.

$$S_i^* = \pm\left[\frac{1}{n}\sum_{i=1}^{n}\left(a_i,\ \mathrm{Th.}\ - a_i,\ \mathrm{Exp.}\ *\right)^2\right]^{\frac{1}{2}} \qquad (16)$$

In this study, 36 experimental data points (n) were considered. Table 3 reveals that according to MIVM, the average relative error and mean standard deviation values are ± 3.10% and 0.0302, respectively. These values are notably lower, indicating the model's precision in predicting the activity of the Zn component in the Zn-Bi-In ternary liquid alloys at 873 K.

Table 3 makes it clear that there are some discrepancies between the theoretical and experimental values [25] of the Zn component's activities in Zn-Bi-In liquid alloys at 873 K, but overall there is reasonable agreement. For the cross-sections $\mathrm{x_{Bi}}$: $\mathrm{x_{In}}$ = 1:2, 8.86% at $\mathrm{x_{Zn}}$ = 0.40160, for $\mathrm{x_{Bi}}$: $\mathrm{x_{In}}$ = 1:1, 3.18% at $\mathrm{x_{Zn}}$ = 0.50040, for $\mathrm{x_{Bi}}$: $\mathrm{x_{In}}$ = 2:1, 8.73% at $\mathrm{x_{Zn}}$ = 0.60090, and for $\mathrm{x_{Bi}}$: $\mathrm{x_{In}}$ = 9: 1, 7.85% at $\mathrm{x_{Zn}}$ = 0.39800 exhibits the highest error measurement, respectively.

Table 4 indicates that the theoretical and experimental [25] values of the excess free energy of mixing in Zn-Bi-In liquid alloys at 873 K exhibit reasonable agreement, albeit with some discrepancies. The highest errors are observed at $\mathrm{x_{Zn}} = 0.1$ for all four cross-sections, specifically $\mathrm{x_{Bi}}$: $\mathrm{x_{In}}$ = 1:2, 1:1, 2:1, and 9:1.

Figure 1(a) demonstrates that there is a significant positive departure from ideality in Zn's theoretical and experimental activity ($\mathrm{a_{Zn}}$). Up to $\mathrm{x_{Zn}}$ = 0.2992, the deviation between the theoretical and experimental results is essentially unchanged. The experimental and theoretical values exhibit a small dispersion in the concentration range of $0.2992 \leq x_{\mathrm{Zn}} \leq 0.4912$. Again, from $\mathrm{x_{Zn}}$ = 0.4912 to 1.0, the deviation between them is minor. In particular, these plots show that, as $\mathrm{x_{Zn}}$ increases within the parameter range of $0.0 \leq x_{\mathrm{Zn}} \leq 0.4016$, there is an increasing positive activity deviation from ideal Raoult's law. On the other hand, a decrease in the positive activity deviation is noted in the range $0.4016 \leq x_{\mathrm{Zn}} \leq 1.0$. These observations are particular to cross-sections with $\mathrm{x_{Bi}}$: $\mathrm{x_{In}}$ = 1:2 as their defining ratio.

For Zn-Bi-In liquid alloys at 873 K, the integral excess free energy of mixing ΔG^{XS} versus $\mathrm{x_{Zn}}$ for the cross-section $\mathrm{x_{Bi}}$: $\mathrm{x_{In}}$ =1:2 was plotted in Figure 1(b). For this cross-section, the data indicates that there were both positive and negative values found for ΔG^{XS}. Under the same concentration, $\mathrm{x_{Zn}}$ = 0.6, the maximum positive values were 2453.4 J/mol (Th.) and 2566.0 J/mol (Expt.). The apparent discrepancy between the theoretical and experimental values of ΔG^{XS} is more noticeable at lower $\mathrm{x_{Zn}}$ concentrations, especially in the concentration range of $0.0 \leq x_{\mathrm{Zn}} \leq 0.5$. On the other hand, the observed difference between them decreases within the concentration range of $0.5 \leq x_{\mathrm{Zn}} \leq 1.0$, suggesting that the two datasets are convergent.

Zn's theoretical and experimental activity shows a notable positive departure from ideality, as shown in Figure 2(a). The difference between the theoretical and experimental results is nearly constant up to $\mathrm{x_{Zn}}$ = 0.3024. In the concentration range of $0.3024 \leq \mathrm{x_{Zn}} \leq 0.5986$, there is a slight dispersion between the theoretical and experimental values. Again, there is not much of a difference between $\mathrm{x_{Zn}}$ = 0.5986 and 1.0. These plots indicate that as $\mathrm{x_{Zn}}$ increases, there is a noticeable increase in the positive activity deviation of Zn from the ideal Raoult's law within the parameter range of $0.0 \leq x_{\mathrm{Zn}} \leq 0.3998$. In contrast, there is a noticeable decline in the positive Zn's activity deviation in the range of $0.3998 \leq x_{\mathrm{Zn}} \leq 1.0$ at the cross-section, $\mathrm{x_{Bi}}$: $\mathrm{x_{In}}$ = 1:1.

The plot of ΔG^{XS} versus $\mathrm{x_{Zn}}$ for the cross-section $\mathrm{x_{Bi}}$: $\mathrm{x_{In}}$ = 1:1, as shown in Figure 2(b),

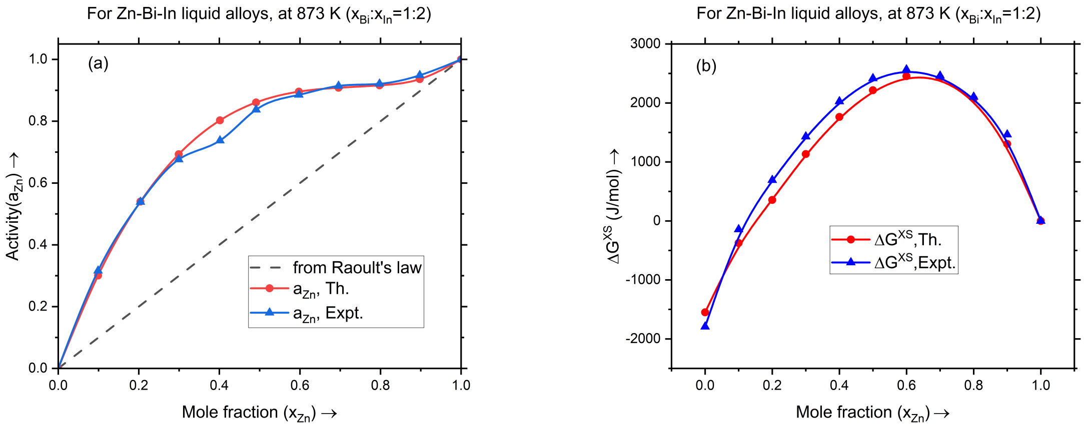

Figure 1: Theoretical and experimental variations of (a) Zn activity with respect to x_{zn} and (b) excess free energy of mixing with respect to x_{zn} presented for Zn-Bi-In liquid alloys at 873 K at the cross-section xBi:xIn =1:2, expt. data taken from the ref. [25].

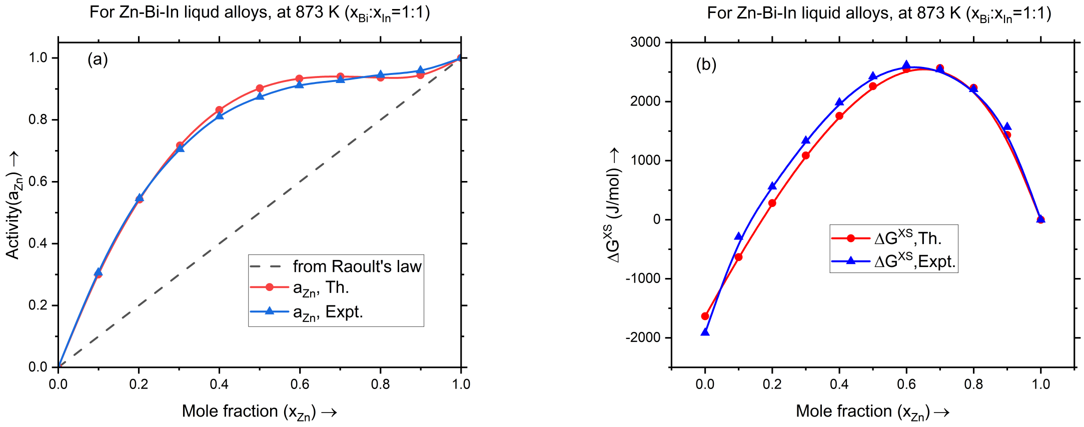

Figure 2: Theoretical and experimental variations of (a) Zn activity with respect to x_{zn} and (b) excess free energy of mixing with respect to x_{zn} presented for Zn-Bi-In liquid alloys at 873 K at the cross-section xBi:xIn =1:1, expt. data taken from the ref. [25].

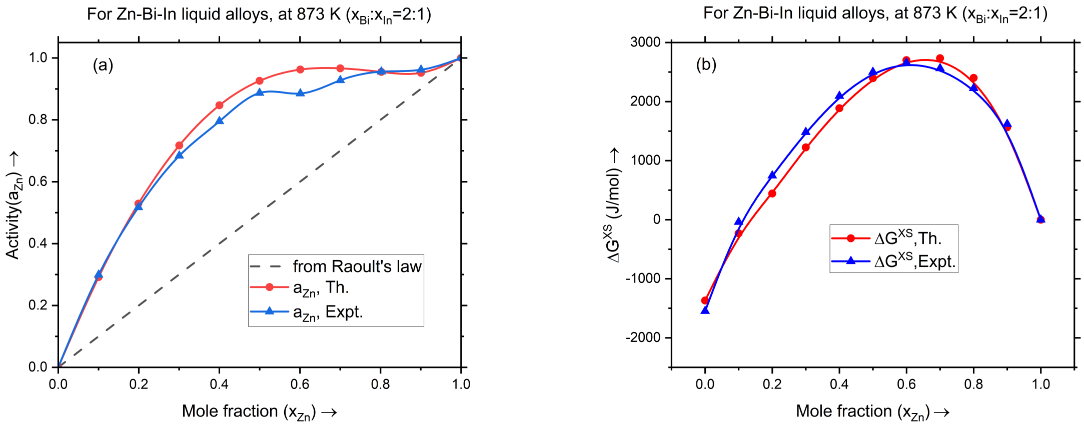

Figure 3: Theoretical and experimental variations of (a) Zn activity with respect to x_{zn} and (b) excess free energy of mixing with respect to x_{zn} presented for Zn-Bi-In liquid alloys at 873 K at the cross-section xBi:xIn =2:1, expt. data taken from the ref. [25].

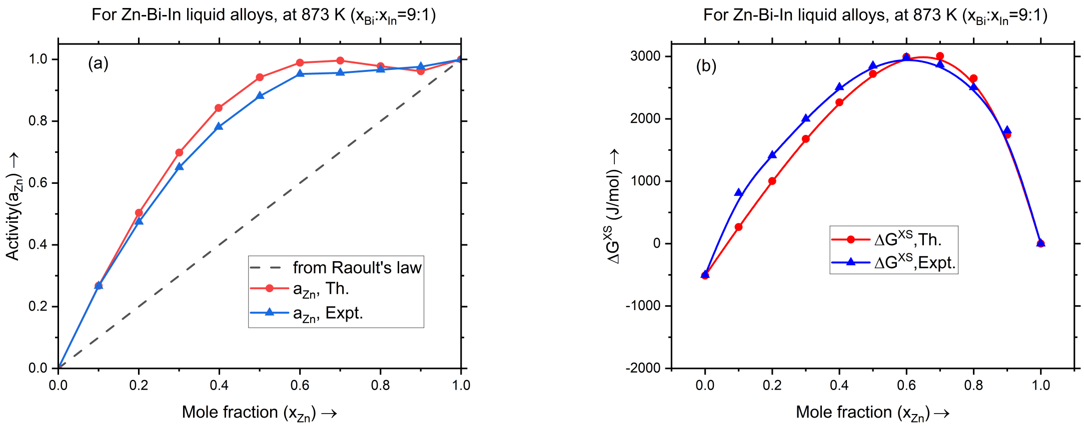

Figure 4: Theoretical and experimental variations of (a) Zn activity with respect to x_{zn} and (b) excess free energy of mixing with respect to x_{zn} presented for Zn-Bi-In liquid alloys at 873 K at the cross-section xBi:xIn =9:1, expt. data taken from the ref. [25].

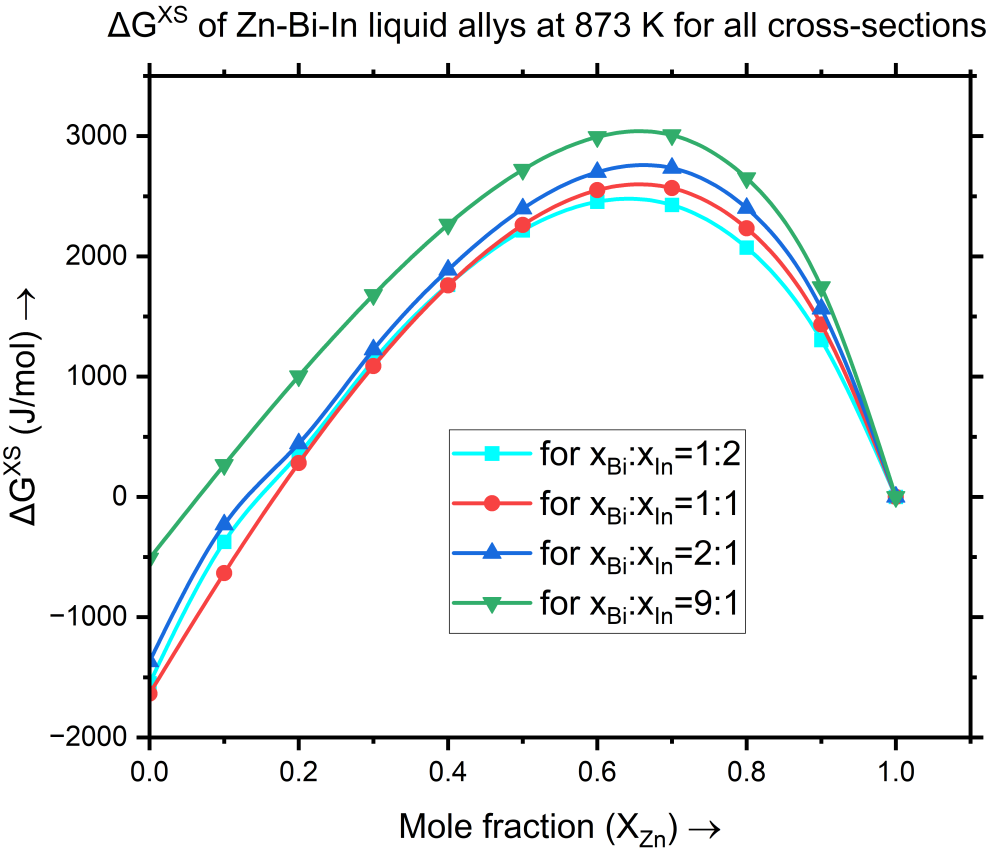

Figure 5: Comparison of excess free energy of mixing with respect to x_{Zn} presented for Zn-Bi-In liquid alloys at 873 K at all the cross-sections, i.e., x_{Bi}: x_{In} =1:2, 1:1, 2:1, and 9:1.

indicates that there were also both positive and negative values found for ΔG^{XS}. Under the concentrations, $\mathrm{x_{Zn}} = 0.7$, the maximum positive theoretical value was 2567.7 J/mol, and the maximum positive experimental value was 2618.0 J/mol at $\mathrm{x_{Zn}} = 0.6$. The difference between the theoretical and experimental ΔG^{XS} values is more noticeable at lower $\mathrm{x_{Zn}}$ concentrations in the range of $0.0 \leq x_{\mathrm{Zn}} \leq 0.5$. On the other hand, convergence occurs in the concentration range $0.5 \leq x_{\mathrm{Zn}} \leq 1.0$.

Figure 3(a) reveals a notable positive departure from ideality in Zn's theoretical and experimental activity. The deviation remains consistent up to $\mathrm{x_{Zn}} = 0.1991$. The dispersion between them is slightly larger in the concentration range of$0.1991 \leq x_{\mathrm{Zn}} \leq 0.4998$. At $\mathrm{x_{Zn}} = 0.6009$, the difference between them is the maximum. Again, from $\mathrm{x_{Zn}} = 0.6009$ to 1.0, the deviation between them becomes smaller. According to these plots, there is a noticeable increase in the positive activity deviation from the ideal Raoult's law as $\mathrm{x_{Zn}}$ increases within the specified parameter range of $0.0 \leq x_{\mathrm{Zn}} \leq 0.4001$. On the other hand, at cross-sections $\mathrm{x_{Bi}}$: $\mathrm{x_{In}} = 2{:}1$, a decrease in positive activity deviation is observed within the following range of $0.4001 \leq x_{\mathrm{Zn}} \leq 1.0$.

As seen in Figure 3(b), the plot of ΔG^{XS} versus $\mathrm{x_{Zn}}$ for the cross-section $\mathrm{x_{Bi}}$: $\mathrm{x_{In}} = 2{:}1$ shows that ΔG^{XS} was also found to have both positive and negative values. The maximum positive values were 2734.2 J/mol (Th.) at $\mathrm{x_{Zn}} = 0.7$ and 2658.0 J/mol (Expt.) at $\mathrm{x_{Zn}} = 0.6$. The disparity in ΔG^{XS} values is pronounced at lower $\mathrm{x_{Zn}}$ concentrations, notably at $0.0 \leq x_{\mathrm{Zn}} \leq 0.4$. Conversely, the difference diminishes at $0.4 \leq x_{\mathrm{Zn}} \leq 0.6$, increases at $0.6 \leq x_{\mathrm{Zn}} \leq 0.8$, and decreases again toward the concentration range's end.

Figure 4(a) illustrates a notable positive departure from ideality in Zn's theoretical and experimental activity. The deviation remains consistent up to $\mathrm{x_{Zn}} = 0.2005$. In the concentration range of $0.3004 \leq x_{\mathrm{Zn}} \leq 0.7002$, the dispersion between them becomes larger. Again, after that, in the range of $0.7002 \leq x_{\mathrm{Zn}} \leq 1.0$, the deviation between them becomes smaller. According to these plots, there is a noticeable increase in the positive activity deviation from the ideal Raoult's law as $\mathrm{x_{Zn}}$ increases within the specified parameter range of $0.0 \leq x_{\mathrm{Zn}} \leq 0.398$. On the other hand, at cross-section $\mathrm{x_{Bi}}$: $\mathrm{x_{In}} = 9{:}1$, a decrease in positive activity deviation is observed within the following range of $0.398 \leq x_{\mathrm{Zn}} \leq 1.0$.

As can be seen in Figure 4(b), the plot of ΔG^{XS} versus $\mathrm{X_{Zn}}$ for the cross-section $\mathrm{x_{Bi}}$: $\mathrm{x_{In}} = 9{:}1$ shows that ΔG^{XS} was also found to have both positive and negative values. The maximum positive values were 3007.9 J/mol (Th.) at $\mathrm{x_{Zn}} = 0.7$ and 2981 J/mol (Expt.) at $\mathrm{x_{Zn}} = 0.6$. The apparent discrepancy between the theoretical and experimental values of ΔG^{XS} is more noticeable at lower $\mathrm{x_{Zn}}$ concentrations, especially in the concentration range of $0.1 \leq x_{\mathrm{Zn}} \leq 0.3$. On the other concentrations of $\mathrm{x_{Zn}}$, the observed difference between them is smaller.

The graphical plots of excess Gibbs free energy of mixing Zn-Bi-In liquid alloys at 873 K for all four cross-sections, i.e., $\mathrm{x_{Bi}}$: $\mathrm{x_{In}}$ =1:2, 1:1, 2:1, and 9:1, have been shown in Figure 5. On comparison, we found that when the molar the ratio of Bi and In increases from $\mathrm{x_{Bi}}$: $\mathrm{x_{In}}$ =1:2 to 9:1, the maximum positive values of ΔG^{XS} increase. Furthermore, keeping the concentration of Zn constant, we observe that in concentrations greater than 0.4, i.e., $\mathrm{x_{Zn}} = 0.5$ to 0.9, in every case, as the ratio ($\mathrm{x_{Bi}}$: $\mathrm{x_{In}}$) increases from 1:2 to 9:1, then the positive values of ΔG^{XS} also increase. For concentrations $\mathrm{x_{Zn}}$ below 0.5, i.e., for each case of $\mathrm{x_{Zn}} = 0.1$, 0.2, 0.3, and 0.4, as the ratio $\mathrm{x_{Bi}}$:$\mathrm{x_{In}}$ increases from 1:2 to 1:1, either the negative value of ΔG^{XS} increases or the positive values of ΔG^{XS} decrease, and afterward, as the ratio $\mathrm{x_{Bi}}$: $\mathrm{x_{In}}$ increases from 1:1 to 9:1, either the negative ΔG^{XS} values decrease or positive ΔG^{XS} values increase. For example, in a particular case, at $\mathrm{x_{zn}} = 0.1$, the negative ΔG^{XS} values have decreased and finally shifted to positive as $\mathrm{x_{Bi}}$: $\mathrm{x_{In}}$ increases from 1:1 to 9:1.

A positive deviation from Raoult's Law, and thus a positive excess Gibbs free energy for all four cross-sections, indicates that the interactions between the components in the mixture are weaker than expected based on ideal behavior. In the context of liquid alloys, a positive deviation in the activity of a component like Zn suggests that the interactions between zinc atoms and the other components (Bi and In in this case) are weaker in the mixture than one would predict from assuming ideal behavior. It also indicates that the partial vapor pressures of the component Zn in Zn-Bi-In alloys at 873 K are higher than their corresponding vapor pressures in the case of an ideal mixture. Furthermore, the positive values of ΔG^{XS} for all three cross-sections indicate that after mixing, the average distance between the molecules of the three liquid metals increases, i.e., the volume of the mixture expands relative to the ideal mixture.

4 Conclusion

The positive deviation of the activities of the component Zn (for the Zn-Bi-In system) at all four cross-sections of Bi and In, i.e., 1:2, 1:1, 2:1, and 9:1 from ideal mixing, has been successfully explained theoretically using MIVM. There is a significant positive departure from ideality in Zn's activity in Zn-Bi-In liquid alloys at all four cross-sections of Bi and In. Similarly, both the negative and positive values of the excess Gibbs free energy of mixing for the Zn-Bi-In system for all four cross-sections of x_{Bi}/x_{In} have also been successfully explained by the same theoretical model. The maximum positive values of ΔG^{XS} increase when the molar ratio of Bi and In increases from 1:2 to 9:1 in the Zn-Bi-In system. Since there is a lack of existing research on the ΔG^{XS} of Zn-Bi-In liquid alloys employing the MIVM model, the theoretical information on the ΔG^{XS} of ternary liquid alloys presented in this study will be valuable for providing a more precise understanding of the thermodynamic characteristics of Zn-Bi-In liquid alloys.

References

[1] HongWei Yang, Bin Yang, BaoQiang Xu, DaChun Liu, and DongPing Tao. Application of molecular interaction volume model in vacuum distillation of pb-based alloys. *Vacuum*, 86(9):1296–1299, 2012.

[2] Dong Ping Tao. Prediction of the coordination numbers of liquid metals. *Metallurgical and materials transactions A*, 36:3495–3497, 2005.

[3] Lingxin Kong, Bin Yang, Baoqiang Xu, and Yifu Li. Application of molecular interaction volume model for phase equilibrium of sn-based binary system in vacuum distillation. *Metallurgical and Materials Transactions A*, 45:4405–4410, 2014.

[4] Ling-Xin Kong, YANG Bin, Bao-Qiang Xu, Yi-fu Li, LI Liang, Da-chun Liu, and Yong-nian Dai. Application of molecular interaction volume model in separation of pb–sn–sb ternary alloy by vacuum distillation. *Transactions of Nonferrous Metals Society of China*, 23(8):2408–2415, 2013.

[5] Mulugeta Abtew and Guna Selvaduray. Lead-free solders in microelectronics. *Materials Science and Engineering: R: Reports*, 27(5-6):95–141, 2000.

[6] Nele Moelans, KC Hari Kumar, and Patrick Wollants. Thermodynamic optimization of the lead-free solder system bi–in–sn–zn. *Journal of alloys and compounds*, 360(1-2):98–106, 2003.

[7] Xing Jun Liu, Tokuro Yamaki, Ikuo Ohnuma, Ryosuke Kainuma, and Kiyohito Ishida. Thermodynamic calculations of phase equilibria, surface tension and viscosity in the in-ag-x (x= bi, sb) system. *Materials Transactions*, 45(3):637–645, 2004.

[8] Sabine Knott and Adolf Mikula. Thermodynamic properties of liquid al-sn-zn alloys: A possible new lead-free solder material. *Materials transactions*, 43(8):1868–1872, 2002.

[9] Sanjay Kumar Sah, Indu Shekhar Jha, and Ishwar Koirala. Theoretical investigation of the thermodynamic properties of lead-free ternary alloys sn-sb-bi and their subsystems. *BMC Journal of Scientific Research*, 6(1):16–30, 2023.

[10] Sanjay Kumar Sah, Indu Shekhar Jha, and Ishwar Koirala. Theoretical examination of some thermodynamic properties in in-bi-sn liquid alloy and its sub-binary systems. *Journal of Electronic Materials*, 52(9):6350–6359, 2023.

[11] Stefano Amore, Enrica Ricci, Tiziana Lanata, and Rada Novakovic. Surface tension and wetting behaviour of molten cu–sn alloys. *Journal of alloys and compounds*, 452(1):161–166, 2008.

[12] Joonho Lee, Wataru Shimoda, and Toshihiro Tanaka. Surface tension and its temperature coefficient of liquid sn-x (x= ag, cu) alloys. *Materials transactions*, 45(9):2864–2870, 2004.

[13] DG Ivey. Microstructural characterization of au/sn solder for packaging in optoelectronic applications. *Micron*, 29(4):281–287, 1998.

[14] YT Lai and CY Liu. Study of wetting reaction between eutectic ausn and au foil. *Journal of electronic materials*, 35:28–34, 2006.

[15] Toshio Takenaka, Satoru Kano, Masanori Kajihara, Noriharu Kurokawa, and Katsuhiko Sakamoto. Growth behavior of au–sn and ag–sn compounds during solid-state reactive diffusion between au–ag alloys and sn. *Materials transactions*, 46(8):1825–1832, 2005.

[16] Kuo-Chih Chou. A general solution model for predicting ternary thermodynamic properties. *Calphad*, 19(3):315–325, 1995.

[17] N Panthi, IB Bhandari, and I Koirala. Thermophysical study of sodium–indium alloy. *Metallofizika i Novejsie Tehnologii*, 44(11), 2022.

[18] Narayan Panthi, Indra Bhandari, and Ishwar Koirala. Thermophysical behavior of mercury-lead liquid alloy. *Papers in physics*, 14:140005–140005, 2022.

[19] Sophie Poizeau and Donald R Sadoway. Application of the molecular interaction volume model (mivm) to calcium-based liquid alloys of systems forming high-melting intermetallics. *Journal of the American Chemical Society*, 135(22):8260–8265, 2013.

[20] Heng Dai and Dong-Ping Tao. Application of the molecular interaction volume model (mivm) and its modified form to organic vapor-liquid equilibria. *Fluid Phase Equilibria*, 484:74–81, 2019.

[21] Lingxin Kong, Bin Yang, Yifu Li, Baoqiang Xu, Dachun Liu, and Guobin Jia. Application of mivm for pb-sn system in vacuum distillation. *Metallurgical and Materials Transactions B*, 43:1649–1656, 2012.

[22] Sanjay Kumar Sah and Ishwar Koirala. Computational assessment of sn activities and integral excess free energy change for mixing in the sn-au-cu ternary liquid alloys using the molecular interaction volume model. *Journal of Physics Communications*, 7(10):105001, 2023.

[23] B Onderka, A Dębski, and W Gąsior. Thermodynamic assessment of the bi-in-zn system. *Archives of Metallurgy and Materials*, 60(2A):567–575, 2015.

[24] Zuoan Li, Sabine Knott, and Adolf Mikula. Calorimetric investigations of liquid bi–in–zn alloys. *Acta materialia*, 55(7):2417–2422, 2007.

[25] Sabine Knott, Zuoan Li, C-H Wang, and Adolf Mikula. Electromotive force measurements in the ternary system bi-in-zn. *Metallurgical and Materials Transactions A*, 41:3130–3135, 2010.

[26] Dong Ping Tao. Prediction of activities of all components in the lead-free solder systems bi–in–sn and bi–in–sn–zn. *Journal of alloys and compounds*, 457(1-2):124–130, 2008.

[27] Dong Ping Tao. A new model of thermodynamics of liquid mixtures and its application to liquid alloys. *Thermochimica Acta*, 363(1-2):105–113, 2000.

[28] Yisau A Odusote, Adewumi I Popoola, Kayode D Adedayo, and Samuel T Ogunjo. Thermodynamic properties of al in ternary lead-free solder al-sn-zn alloys. *Materials Science-Poland*, 35(3):583–593, 2017.

[29] Dong Ping Tao. Prediction of the thermodynamic properties of multicomponent liquid alloys by binary infinite dilute activity coefficients. *Metallurgical and Materials Transactions*, 32(6):1205, 2001.

[30] Roderick IL Guthrie. The physical properties of liquid metals. *(No Title)*, 1987.